

BABAR-PUB-03/001
SLAC-PUB-9644

Measurement of $B^0 \rightarrow D_s^{(*)+} D^{*-}$ Branching Fractions and $B^0 \rightarrow D_s^{*+} D^{*-}$ Polarization with a Partial Reconstruction Technique

B. Aubert,¹ R. Barate,¹ D. Boutigny,¹ J.-M. Gaillard,¹ A. Hicheur,¹ Y. Karyotakis,¹ J. P. Lees,¹ P. Robbe,¹ V. Tisserand,¹ A. Zghiche,¹ A. Palano,² A. Pompili,² J. C. Chen,³ N. D. Qi,³ G. Rong,³ P. Wang,³ Y. S. Zhu,³ G. Eigen,⁴ I. Ofte,⁴ B. Stugu,⁴ G. S. Abrams,⁵ A. W. Borgland,⁵ A. B. Breon,⁵ D. N. Brown,⁵ J. Button-Shafer,⁵ R. N. Cahn,⁵ E. Charles,⁵ M. S. Gill,⁵ A. V. Gritsan,⁵ Y. Groysman,⁵ R. G. Jacobsen,⁵ R. W. Kadel,⁵ J. Kadyk,⁵ L. T. Kerth,⁵ Yu. G. Kolomensky,⁵ J. F. Kral,⁵ C. LeClerc,⁵ M. E. Levi,⁵ G. Lynch,⁵ L. M. Mir,⁵ P. J. Oddone,⁵ T. J. Orimoto,⁵ M. Pripstein,⁵ N. A. Roe,⁵ A. Romosan,⁵ M. T. Ronan,⁵ V. G. Shelkov,⁵ A. V. Telnov,⁵ W. A. Wenzel,⁵ T. J. Harrison,⁶ C. M. Hawkes,⁶ D. J. Knowles,⁶ S. W. O'Neale,⁶ R. C. Penny,⁶ A. T. Watson,⁶ N. K. Watson,⁶ T. Deppermann,⁷ K. Goetzen,⁷ H. Koch,⁷ B. Lewandowski,⁷ M. Pelizaeus,⁷ K. Peters,⁷ H. Schmuecker,⁷ M. Steinke,⁷ N. R. Barlow,⁸ W. Bhimji,⁸ J. T. Boyd,⁸ N. Chevalier,⁸ P. J. Clark,⁸ W. N. Cottingham,⁸ C. Mackay,⁸ F. F. Wilson,⁸ C. Hearty,⁹ T. S. Mattison,⁹ J. A. McKenna,⁹ D. Thiessen,⁹ S. Jolly,¹⁰ P. Kyberd,¹⁰ A. K. McKemey,¹⁰ V. E. Blinov,¹¹ A. D. Bukin,¹¹ V. B. Golubev,¹¹ V. N. Ivanchenko,¹¹ E. A. Kravchenko,¹¹ A. P. Onuchin,¹¹ S. I. Serednyakov,¹¹ Yu. I. Skovpen,¹¹ A. N. Yushkov,¹¹ D. Best,¹² M. Chao,¹² D. Kirkby,¹² A. J. Lankford,¹² M. Mandelkern,¹² S. McMahon,¹² R. K. Mommson,¹² W. Roethel,¹² D. P. Stoker,¹² K. Arisaka,¹³ C. Buchanan,¹³ H. K. Hadavand,¹⁴ E. J. Hill,¹⁴ D. B. MacFarlane,¹⁴ H. P. Paar,¹⁴ Sh. Rahatlou,¹⁴ G. Raven,¹⁴ U. Schwanke,¹⁴ V. Sharma,¹⁴ J. W. Berryhill,¹⁵ C. Campagnari,¹⁵ B. Dahmes,¹⁵ N. Kuznetsova,¹⁵ S. L. Levy,¹⁵ O. Long,¹⁵ A. Lu,¹⁵ M. A. Mazur,¹⁵ J. D. Richman,¹⁵ W. Verkerke,¹⁵ J. Beringer,¹⁶ A. M. Eisner,¹⁶ C. A. Heusch,¹⁶ W. S. Lockman,¹⁶ T. Schalk,¹⁶ R. E. Schmitz,¹⁶ B. A. Schumm,¹⁶ A. Seiden,¹⁶ M. Turri,¹⁶ W. Walkowiak,¹⁶ D. C. Williams,¹⁶ M. G. Wilson,¹⁶ J. Albert,¹⁷ E. Chen,¹⁷ G. P. Dubois-Felsmann,¹⁷ A. Dvoretzki,¹⁷ D. G. Hitlin,¹⁷ I. Narsky,¹⁷ F. C. Porter,¹⁷ A. Ryd,¹⁷ A. Samuel,¹⁷ S. Yang,¹⁷ S. Jayatilleke,¹⁸ G. Mancinelli,¹⁸ B. T. Meadows,¹⁸ M. D. Sokoloff,¹⁸ T. Barillari,¹⁹ F. Blanc,¹⁹ P. Bloom,¹⁹ W. T. Ford,¹⁹ U. Nauenberg,¹⁹ A. Olivas,¹⁹ P. Rankin,¹⁹ J. Roy,¹⁹ J. G. Smith,¹⁹ W. C. van Hoek,¹⁹ L. Zhang,¹⁹ J. L. Harton,²⁰ T. Hu,²⁰ A. Soffer,²⁰ W. H. Toki,²⁰ R. J. Wilson,²⁰ J. Zhang,²⁰ D. Altenburg,²¹ T. Brandt,²¹ J. Brose,²¹ T. Colberg,²¹ M. Dickopp,²¹ R. S. Dubitzky,²¹ A. Hauke,²¹ H. M. Lacker,²¹ E. Maly,²¹ R. Müller-Pfefferkorn,²¹ R. Nogowski,²¹ S. Otto,²¹ K. R. Schubert,²¹ R. Schwierz,²¹ B. Spaan,²¹ L. Wilden,²¹ D. Bernard,²² G. R. Bonneaud,²² F. Brochard,²² J. Cohen-Tanugi,²² S. T'Jampens,²² Ch. Thiebaux,²² G. Vasileiadis,²² M. Verderi,²² A. Anjomshoa,²³ R. Bernet,²³ A. Khan,²³ D. Lavin,²³ F. Muheim,²³ S. Playfer,²³ J. E. Swain,²³ J. Tinslay,²³ C. Borean,²⁴ C. Bozzi,²⁴ L. Piemontese,²⁴ A. Sarti,²⁴ E. Treadwell,²⁵ F. Anulli,²⁶ * R. Baldini-Ferroli,²⁶ A. Calcaterra,²⁶ R. de Sangro,²⁶ D. Falciari,²⁶ G. Finocchiaro,²⁶ P. Patteri,²⁶ I. M. Peruzzi,²⁶ * M. Piccolo,²⁶ A. Zallo,²⁶ S. Bagnasco,²⁷ A. Buzzo,²⁷ R. Contri,²⁷ G. Crosetti,²⁷ M. Lo Vetere,²⁷ M. Macri,²⁷ M. R. Monge,²⁷ S. Passaggio,²⁷ F. C. Pastore,²⁷ C. Patrignani,²⁷ E. Robutti,²⁷ A. Santroni,²⁷ S. Tosi,²⁷ S. Bailey,²⁸ M. Morii,²⁸ G. J. Grenier,²⁹ S.-J. Lee,²⁹ U. Mallik,²⁹ J. Cochran,³⁰ H. B. Crawley,³⁰ J. Lamsa,³⁰ W. T. Meyer,³⁰ S. Prell,³⁰ E. I. Rosenberg,³⁰ J. Yi,³⁰ M. Davier,³¹ G. Grosdidier,³¹ A. Höcker,³¹ S. Laplace,³¹ F. Le Diberder,³¹ V. Lepeltier,³¹ A. M. Lutz,³¹ T. C. Petersen,³¹ S. Plaszczynski,³¹ M. H. Schune,³¹ L. Tantot,³¹ G. Wormser,³¹ R. M. Bionta,³² V. Brigljević,³² C. H. Cheng,³² D. J. Lange,³² K. van Bibber,³² D. M. Wright,³² A. J. Bevan,³³ J. R. Fry,³³ E. Gabathuler,³³ R. Gamet,³³ M. Kay,³³ D. J. Payne,³³ R. J. Sloane,³³ C. Touramanis,³³ M. L. Aspinwall,³⁴ D. A. Bowerman,³⁴ P. D. Dauncey,³⁴ U. Egede,³⁴ I. Eschrich,³⁴ G. W. Morton,³⁴ J. A. Nash,³⁴ P. Sanders,³⁴ G. P. Taylor,³⁴ J. J. Back,³⁵ G. Bellodi,³⁵ P. Dixon,³⁵ P. F. Harrison,³⁵ H. W. Shorthouse,³⁵ P. Strother,³⁵ P. B. Vidal,³⁵ G. Cowan,³⁶ H. U. Flaecher,³⁶ S. George,³⁶ M. G. Green,³⁶ A. Kurup,³⁶ C. E. Marker,³⁶ T. R. McMahon,³⁶ S. Ricciardi,³⁶ F. Salvatore,³⁶ G. Vaitsas,³⁶ M. A. Winter,³⁶ D. Brown,³⁷ C. L. Davis,³⁷ J. Allison,³⁸ R. J. Barlow,³⁸ A. C. Forti,³⁸ P. A. Hart,³⁸ F. Jackson,³⁸ G. D. Lafferty,³⁸ A. J. Lyon,³⁸ J. H. Weatherall,³⁸ J. C. Williams,³⁸ A. Farbin,³⁹ A. Jawahery,³⁹ V. Lillard,³⁹ D. A. Roberts,³⁹ G. Blaylock,⁴⁰ C. Dallapiccola,⁴⁰ K. T. Flood,⁴⁰ S. S. Hertzbach,⁴⁰ R. Kofler,⁴⁰ V. B. Koptchev,⁴⁰ T. B. Moore,⁴⁰ H. Staengle,⁴⁰ S. Willocq,⁴⁰ R. Cowan,⁴¹ G. Sciolla,⁴¹ F. Taylor,⁴¹ R. K. Yamamoto,⁴¹ D. J. J. Mangeol,⁴² M. Milek,⁴² P. M. Patel,⁴² F. Palombo,⁴³ J. M. Bauer,⁴⁴ L. Cremaldi,⁴⁴ V. Eschenburg,⁴⁴ R. Kroeger,⁴⁴ J. Reidy,⁴⁴ D. A. Sanders,⁴⁴ D. J. Summers,⁴⁴ H. W. Zhao,⁴⁴ C. Hast,⁴⁵ P. Taras,⁴⁵ H. Nicholson,⁴⁶ C. Cartaro,⁴⁷ N. Cavallo,⁴⁷ G. De Nardo,⁴⁷ F. Fabozzi,⁴⁷ † C. Gatto,⁴⁷ L. Lista,⁴⁷ P. Paolucci,⁴⁷ D. Piccolo,⁴⁷ C. Sciacca,⁴⁷ J. M. LoSecco,⁴⁸ T. A. Gabriel,⁴⁹ B. Brau,⁵⁰ T. Pulliam,⁵⁰ J. Brau,⁵¹ R. Frey,⁵¹ M. Iwasaki,⁵¹ C. T. Potter,⁵¹

arXiv:hep-ex/0302015v1 13 Feb 2003

N. B. Sinev,⁵¹ D. Strom,⁵¹ E. Torrence,⁵¹ F. Colecchia,⁵² A. Dorigo,⁵² F. Galeazzi,⁵² M. Margoni,⁵² M. Morandin,⁵² M. Posocco,⁵² M. Rotondo,⁵² F. Simonetto,⁵² R. Stroili,⁵² G. Tiozzo,⁵² C. Voci,⁵² M. Benayoun,⁵³ H. Briand,⁵³ J. Chauveau,⁵³ P. David,⁵³ Ch. de la Vaissière,⁵³ L. Del Buono,⁵³ O. Hamon,⁵³ Ph. Leruste,⁵³ J. Ocariz,⁵³ M. Pivk,⁵³ L. Roos,⁵³ J. Stark,⁵³ P. F. Manfredi,⁵⁴ V. Re,⁵⁴ V. Speziali,⁵⁴ L. Gladney,⁵⁵ Q. H. Guo,⁵⁵ J. Panetta,⁵⁵ C. Angelini,⁵⁶ G. Batignani,⁵⁶ S. Bettarini,⁵⁶ M. Bondioli,⁵⁶ F. Bucci,⁵⁶ G. Calderini,⁵⁶ E. Campagna,⁵⁶ M. Carpinelli,⁵⁶ F. Forti,⁵⁶ M. A. Giorgi,⁵⁶ A. Lusiani,⁵⁶ G. Marchiori,⁵⁶ F. Martinez-Vidal,⁵⁶ M. Morganti,⁵⁶ N. Neri,⁵⁶ E. Paoloni,⁵⁶ M. Rama,⁵⁶ G. Rizzo,⁵⁶ F. Sandrelli,⁵⁶ G. Triggiani,⁵⁶ J. Walsh,⁵⁶ M. Haire,⁵⁷ D. Judd,⁵⁷ K. Paick,⁵⁷ D. E. Wagoner,⁵⁷ N. Danielson,⁵⁸ P. Elmer,⁵⁸ C. Lu,⁵⁸ V. Miftakov,⁵⁸ J. Olsen,⁵⁸ A. J. S. Smith,⁵⁸ A. Tumanov,⁵⁸ E. W. Varnes,⁵⁸ F. Bellini,⁵⁹ G. Cavoto,^{58,59} D. del Re,⁵⁹ R. Faccini,^{14,59} F. Ferrarotto,⁵⁹ F. Ferroni,⁵⁹ M. Gaspero,⁵⁹ E. Leonardi,⁵⁹ M. A. Mazzoni,⁵⁹ S. Morganti,⁵⁹ M. Pierini,⁵⁹ G. Piredda,⁵⁹ F. Safai Tehrani,⁵⁹ M. Serra,⁵⁹ C. Voena,⁵⁹ S. Christ,⁶⁰ G. Wagner,⁶⁰ R. Waldi,⁶⁰ T. Adye,⁶¹ N. De Groot,⁶¹ B. Franek,⁶¹ N. I. Geddes,⁶¹ G. P. Gopal,⁶¹ E. O. Olaiya,⁶¹ S. M. Xella,⁶¹ R. Aleksan,⁶² S. Emery,⁶² A. Gaidot,⁶² S. F. Ganzhur,⁶² P.-F. Giraud,⁶² G. Hamel de Monchenault,⁶² W. Kozanecki,⁶² M. Langer,⁶² G. W. London,⁶² B. Mayer,⁶² G. Schott,⁶² B. Serfass,⁶² G. Vasseur,⁶² Ch. Yeche,⁶² M. Zito,⁶² M. V. Purohit,⁶³ A. W. Weidemann,⁶³ F. X. Yumiceva,⁶³ K. Abe,⁶⁴ D. Aston,⁶⁴ R. Bartoldus,⁶⁴ N. Berger,⁶⁴ A. M. Boyarski,⁶⁴ O. L. Buchmueller,⁶⁴ M. R. Convery,⁶⁴ D. P. Coupal,⁶⁴ D. Dong,⁶⁴ J. Dorfan,⁶⁴ W. Dunwoodie,⁶⁴ R. C. Field,⁶⁴ T. Glanzman,⁶⁴ S. J. Gowdy,⁶⁴ E. Grauges-Pous,⁶⁴ T. Hadig,⁶⁴ V. Halyo,⁶⁴ T. Himel,⁶⁴ T. Hryn'ova,⁶⁴ W. R. Innes,⁶⁴ C. P. Jessop,⁶⁴ M. H. Kelsey,⁶⁴ P. Kim,⁶⁴ M. L. Kocian,⁶⁴ U. Langenegger,⁶⁴ D. W. G. S. Leith,⁶⁴ S. Luitz,⁶⁴ V. Luth,⁶⁴ H. L. Lynch,⁶⁴ H. Marsiske,⁶⁴ S. Menke,⁶⁴ R. Messner,⁶⁴ D. R. Muller,⁶⁴ C. P. O'Grady,⁶⁴ V. E. Ozcan,⁶⁴ A. Perazzo,⁶⁴ M. Perl,⁶⁴ S. Petrak,⁶⁴ B. N. Ratcliff,⁶⁴ S. H. Robertson,⁶⁴ A. Roodman,⁶⁴ A. A. Salnikov,⁶⁴ T. Schietinger,⁶⁴ R. H. Schindler,⁶⁴ J. Schwiening,⁶⁴ G. Simi,⁶⁴ A. Snyder,⁶⁴ A. Soha,⁶⁴ J. Stelzer,⁶⁴ D. Su,⁶⁴ M. K. Sullivan,⁶⁴ H. A. Tanaka,⁶⁴ J. Va'vra,⁶⁴ S. R. Wagner,⁶⁴ M. Weaver,⁶⁴ A. J. R. Weinstein,⁶⁴ W. J. Wisniewski,⁶⁴ D. H. Wright,⁶⁴ C. C. Young,⁶⁴ P. R. Burchat,⁶⁵ T. I. Meyer,⁶⁵ C. Roat,⁶⁵ W. Bugg,⁶⁶ M. Krishnamurthy,⁶⁶ S. M. Spanier,⁶⁶ J. M. Izen,⁶⁷ I. Kitayama,⁶⁷ X. C. Lou,⁶⁷ F. Bianchi,⁶⁸ M. Bona,⁶⁸ D. Gamba,⁶⁸ L. Bosisio,⁶⁹ G. Della Ricca,⁶⁹ S. Dittongo,⁶⁹ L. Lanceri,⁶⁹ P. Poropat,⁶⁹ L. Vitale,⁶⁹ G. Vuagnin,⁶⁹ R. Henderson,⁷⁰ R. S. Panvini,⁷¹ Sw. Banerjee,⁷² C. M. Brown,⁷² D. Fortin,⁷² P. D. Jackson,⁷² R. Kowalewski,⁷² J. M. Roney,⁷² H. R. Band,⁷³ S. Dasu,⁷³ M. Datta,⁷³ A. M. Eichenbaum,⁷³ H. Hu,⁷³ J. R. Johnson,⁷³ R. Liu,⁷³ F. Di Lodovico,⁷³ A. K. Mohapatra,⁷³ Y. Pan,⁷³ R. Prepost,⁷³ S. J. Sekula,⁷³ J. H. von Wimmersperg-Toeller,⁷³ J. Wu,⁷³ S. L. Wu,⁷³ Z. Yu,⁷³ and H. Neal⁷⁴

(The BABAR Collaboration)

¹Laboratoire de Physique des Particules, F-74941 Annecy-le-Vieux, France

²Università di Bari, Dipartimento di Fisica and INFN, I-70126 Bari, Italy

³Institute of High Energy Physics, Beijing 100039, China

⁴University of Bergen, Inst. of Physics, N-5007 Bergen, Norway

⁵Lawrence Berkeley National Laboratory and University of California, Berkeley, CA 94720, USA

⁶University of Birmingham, Birmingham, B15 2TT, United Kingdom

⁷Ruhr Universität Bochum, Institut für Experimentalphysik 1, D-44780 Bochum, Germany

⁸University of Bristol, Bristol BS8 1TL, United Kingdom

⁹University of British Columbia, Vancouver, BC, Canada V6T 1Z1

¹⁰Brunel University, Uxbridge, Middlesex UB8 3PH, United Kingdom

¹¹Budker Institute of Nuclear Physics, Novosibirsk 630090, Russia

¹²University of California at Irvine, Irvine, CA 92697, USA

¹³University of California at Los Angeles, Los Angeles, CA 90024, USA

¹⁴University of California at San Diego, La Jolla, CA 92093, USA

¹⁵University of California at Santa Barbara, Santa Barbara, CA 93106, USA

¹⁶University of California at Santa Cruz, Institute for Particle Physics, Santa Cruz, CA 95064, USA

¹⁷California Institute of Technology, Pasadena, CA 91125, USA

¹⁸University of Cincinnati, Cincinnati, OH 45221, USA

¹⁹University of Colorado, Boulder, CO 80309, USA

²⁰Colorado State University, Fort Collins, CO 80523, USA

²¹Technische Universität Dresden, Institut für Kern- und Teilchenphysik, D-01062 Dresden, Germany

²²Ecole Polytechnique, LLR, F-91128 Palaiseau, France

²³University of Edinburgh, Edinburgh EH9 3JZ, United Kingdom

²⁴Università di Ferrara, Dipartimento di Fisica and INFN, I-44100 Ferrara, Italy

²⁵Florida A&M University, Tallahassee, FL 32307, USA

²⁶Laboratori Nazionali di Frascati dell'INFN, I-00044 Frascati, Italy

²⁷Università di Genova, Dipartimento di Fisica and INFN, I-16146 Genova, Italy

²⁸Harvard University, Cambridge, MA 02138, USA

- ²⁹University of Iowa, Iowa City, IA 52242, USA
³⁰Iowa State University, Ames, IA 50011-3160, USA
³¹Laboratoire de l'Accélérateur Linéaire, F-91898 Orsay, France
³²Lawrence Livermore National Laboratory, Livermore, CA 94550, USA
³³University of Liverpool, Liverpool L69 3BX, United Kingdom
³⁴University of London, Imperial College, London, SW7 2BW, United Kingdom
³⁵Queen Mary, University of London, E1 4NS, United Kingdom
³⁶University of London, Royal Holloway and Bedford New College, Egham, Surrey TW20 0EX, United Kingdom
³⁷University of Louisville, Louisville, KY 40292, USA
³⁸University of Manchester, Manchester M13 9PL, United Kingdom
³⁹University of Maryland, College Park, MD 20742, USA
⁴⁰University of Massachusetts, Amherst, MA 01003, USA
⁴¹Massachusetts Institute of Technology, Laboratory for Nuclear Science, Cambridge, MA 02139, USA
⁴²McGill University, Montréal, QC, Canada H3A 2T8
⁴³Università di Milano, Dipartimento di Fisica and INFN, I-20133 Milano, Italy
⁴⁴University of Mississippi, University, MS 38677, USA
⁴⁵Université de Montréal, Laboratoire René J. A. Lévesque, Montréal, QC, Canada H3C 3J7
⁴⁶Mount Holyoke College, South Hadley, MA 01075, USA
⁴⁷Università di Napoli Federico II, Dipartimento di Scienze Fisiche and INFN, I-80126, Napoli, Italy
⁴⁸University of Notre Dame, Notre Dame, IN 46556, USA
⁴⁹Oak Ridge National Laboratory, Oak Ridge, TN 37831, USA
⁵⁰Ohio State University, Columbus, OH 43210, USA
⁵¹University of Oregon, Eugene, OR 97403, USA
⁵²Università di Padova, Dipartimento di Fisica and INFN, I-35131 Padova, Italy
⁵³Universités Paris VI et VII, Lab de Physique Nucléaire H. E., F-75252 Paris, France
⁵⁴Università di Pavia, Dipartimento di Elettronica and INFN, I-27100 Pavia, Italy
⁵⁵University of Pennsylvania, Philadelphia, PA 19104, USA
⁵⁶Università di Pisa, Dipartimento di fisica, Scuola Normale Superiore and INFN, I-56010 Pisa, Italy
⁵⁷Prairie View A&M University, Prairie View, TX 77446, USA
⁵⁸Princeton University, Princeton, NJ 08544, USA
⁵⁹Università di Roma La Sapienza, Dipartimento di Fisica and INFN, I-00185 Roma, Italy
⁶⁰Universität Rostock, D-18051 Rostock, Germany
⁶¹Rutherford Appleton Laboratory, Chilton, Didcot, Oxon, OX11 0QX, United Kingdom
⁶²DAPNIA, Commissariat à l'Energie Atomique/Saclay, F-91191 Gif-sur-Yvette, France
⁶³University of South Carolina, Columbia, SC 29208, USA
⁶⁴Stanford Linear Accelerator Center, Stanford, CA 94309, USA
⁶⁵Stanford University, Stanford, CA 94305-4060, USA
⁶⁶University of Tennessee, Knoxville, TN 37996, USA
⁶⁷University of Texas at Dallas, Richardson, TX 75083, USA
⁶⁸Università di Torino, Dipartimento di Fisica Sperimentale and INFN, I-10125 Torino, Italy
⁶⁹Università di Trieste, Dipartimento di Fisica and INFN, I-34127 Trieste, Italy
⁷⁰TRIUMF, Vancouver, BC, Canada V6T 2A3
⁷¹Vanderbilt University, Nashville, TN 37235, USA
⁷²University of Victoria, Victoria, BC, Canada V8W 3P6
⁷³University of Wisconsin, Madison, WI 53706, USA
⁷⁴Yale University, New Haven, CT 06511, USA

(Dated: September 30, 2017)

We present a study of the decays $B^0 \rightarrow D_s^{(*)+} D^{*-}$, using 20.8 fb^{-1} of e^+e^- annihilation data recorded with the BABAR detector. The analysis is conducted with a partial reconstruction technique, in which only the $D_s^{(*)+}$ and the soft pion from the D^{*-} decay are reconstructed. We measure the branching fractions $\mathcal{B}(B^0 \rightarrow D_s^+ D^{*-}) = (1.03 \pm 0.14 \pm 0.13 \pm 0.26)\%$ and $\mathcal{B}(B^0 \rightarrow D_s^{*+} D^{*-}) = (1.97 \pm 0.15 \pm 0.30 \pm 0.49)\%$, where the first error is statistical, the second is systematic, and the third is the error due to the $D_s^+ \rightarrow \phi\pi^+$ branching fraction uncertainty. From the $B^0 \rightarrow D_s^{*+} D^{*-}$ angular distributions, we measure the fraction of longitudinal polarization $\Gamma_L/\Gamma = (51.9 \pm 5.0 \pm 2.8)\%$, which is consistent with theoretical predictions based on factorization.

PACS numbers: 13.25.Hw, 13.25.-k, 14.40.Nd

*Also with Università di Perugia, Perugia, Italy

†Also with Università della Basilicata, Potenza, Italy

I. INTRODUCTION

Precise knowledge of the branching fractions of exclusive B decay modes provides a test of the factorization approach [1]. Factorization neglects final state interactions between the quarks of the two final state mesons. The pattern of branching fractions for two-body B decays to modes such as $D^{(*)}\pi$, $D^{(*)}\rho$ [2] can be successfully accommodated in such a model. However, it is possible that the factorization assumption is not applicable to the decays $B \rightarrow D^{(*)}X$, where the meson X contains a heavy quark. The current experimental uncertainties for $B \rightarrow D_s^{(*)+}\bar{D}^*$ branching fractions [3] do not allow us to perform a precise test of the factorization approach in this case.

Further tests of factorization are provided by measuring the polarization in decays of B mesons to vector-vector final states. Within experimental errors, polarization measurements are consistent with factorization predictions for the final states $\bar{D}^*\rho$ [4], $\bar{D}^*\rho(1450)$ [5], and $D_s^*\bar{D}^*$ [6].

In this paper we present measurements of the branching fractions¹ $\mathcal{B}(B^0 \rightarrow D_s^{(*)+}D^{*-})$. We also report a measurement of the D_s^{*+} polarization in the decay $B^0 \rightarrow D_s^{*+}D^{*-}$, obtained from an angular analysis. These results provide tests of factorization with increased precision.

II. THE BABAR DETECTOR AND DATA SET

The data used in this analysis were collected with the *BABAR* detector at the PEP-II storage ring. An integrated luminosity of 20.8fb^{-1} was recorded in 1999 and 2000 at the $\Upsilon(4S)$ resonance, corresponding to about 22.7 million produced $B\bar{B}$ pairs.

A detailed description of the *BABAR* detector is presented in Ref. [7]. Only the components of the detector most relevant to this analysis are briefly described here. Charged particles are reconstructed with a five-layer, double-sided silicon vertex tracker (SVT) and a 40-layer drift chamber (DCH) with a helium-based gas mixture, placed in a 1.5 T solenoidal field produced by a superconducting magnet. The charged particle resolution is approximately $(\delta p_T/p_T)^2 = (0.0013 p_T)^2 + (0.0045)^2$, where p_T is the transverse momentum given in GeV/ c . The SVT, with a typical single-hit resolution of $10\ \mu\text{m}$, provides measurement of the impact parameters of charged particle tracks in both the plane transverse to the beam direction and along the beam. Charged particle types are identified from the ionization energy loss (dE/dx)

measured in the DCH and SVT, and the Cherenkov radiation detected in a ring imaging Cherenkov device (DIRC). Photons are identified by a CsI(Tl) electromagnetic calorimeter (EMC) with an energy resolution $\sigma(E)/E = 0.023 \cdot (E/\text{GeV})^{-1/4} \oplus 0.019$.

III. METHOD OF PARTIAL RECONSTRUCTION

In selecting candidates for the decays $B^0 \rightarrow D_s^{(*)+}D^{*-}$ with $D^{*-} \rightarrow \bar{D}^0\pi^-$, no attempt is made to reconstruct the \bar{D}^0 decays. Only the $D_s^{(*)+}$ and the soft π^- from the D^{*-} decay are detected. In this way, the candidate selection efficiency is higher by almost an order of magnitude than that obtained with full reconstruction of the final state. Given the four-momenta of the $D_s^{(*)+}$ and π^- , and assuming they originate from a $B^0 \rightarrow D_s^{(*)+}D^{*-}$ decay, the four-momentum of the B^0 can be calculated up to an unknown azimuthal angle ϕ around the $D_s^{(*)+}$ flight direction. This calculation uses the constraint of the known center-of-mass (CM) energy and the masses of the B^0 and D^{*-} mesons. Energy and momentum conservation then allows a determination of the four-momentum of the \bar{D}^0 , whose square yields the ϕ -dependent missing mass

$$M_{\text{miss}} = \sqrt{(\mathbf{P}_B - \mathbf{P}_{D_s^{(*)+}} - \mathbf{P}_\pi)^2}, \quad (1)$$

where \mathbf{P}_B , $\mathbf{P}_{D_s^{(*)+}}$ and \mathbf{P}_π are the four-momenta of the B^0 , $D_s^{(*)+}$ and the soft pion, respectively. In this analysis the missing mass is defined with an arbitrary choice for the angle ϕ , such that the B^0 momentum \mathbf{p}_B makes the smallest possible angle with \mathbf{p}_π and $\mathbf{p}_{D_s^{(*)+}}$ in the CM frame.

IV. EVENT SELECTION

For each event, we calculate the ratio of the second to the zeroth order Fox-Wolfram moments, using all observed charged tracks and neutral clusters. This ratio is required to be less than 0.35 in order to suppress continuum $e^+e^- \rightarrow q\bar{q}$ events, where $q = u, d, s, c$.

We reconstruct D_s^+ mesons in the decay modes $D_s^+ \rightarrow \phi\pi^+$, $D_s^+ \rightarrow \bar{K}^{*0}K^+$ and $D_s^+ \rightarrow K_s^0K^+$, with subsequent decays $\phi \rightarrow K^+K^-$, $\bar{K}^{*0} \rightarrow K^-\pi^+$ and $K_s^0 \rightarrow \pi^+\pi^-$. These modes are selected since they offer the best combination of large branching fraction, good detection efficiency, and high signal-to-background ratio. Charged tracks from the D_s^+ are required to originate from within ± 10 cm along the beam direction and ± 1.5 cm in the transverse plane, and leave at least 12 hits in the DCH.

Kaons are identified using dE/dx information from the SVT and DCH, as well as the Cherenkov angle and the number of photons measured with the DIRC. For each detector component $d = \{\text{SVT}, \text{DCH}, \text{DIRC}\}$, a likelihood L_d^K (L_d^π) is calculated given the kaon (pion) mass

[1] Reference to a specific decay channel or state also implies the charge conjugate decay or state. The notation $D_s^{(*)+}$ refers to either D_s^+ or D_s^{*+} .

hypothesis. A charged particle is classified as a ‘‘loose’’ kaon if it satisfies $L_d^K/L_d^\pi > 1$ for at least one of the detector components. A ‘‘tight’’ kaon classification is made if the condition $\prod_d L_d^K/L_d^\pi > 1$ is satisfied.

Three charged tracks consistent with originating from a common vertex are combined to form a D_s^+ candidate.

In the case of the decay $D_s^+ \rightarrow \phi\pi^+$, two oppositely charged tracks must be identified as kaons with both satisfying the loose criterion, and at least one, the tight criterion. No identification requirement is applied to the pion. The reconstructed invariant mass of the K^+K^- candidates must be within $8 \text{ MeV}/c^2$ of the nominal ϕ mass [8]. In the decay $D_s^+ \rightarrow \phi\pi^+$, the ϕ meson is polarized longitudinally, resulting in the kaons having a $\cos^2\theta_H$ distribution, where θ_H is the angle between the K^+ and D_s^+ directions in the ϕ rest frame. We require $|\cos\theta_H| > 0.3$, which retains 97% of the signal while rejecting about 30% of the background.

In the reconstruction of the $D_s^+ \rightarrow \bar{K}^{*0}K^+$ mode, the $K^-\pi^+$ invariant mass is required to be within $65 \text{ MeV}/c^2$ of the nominal \bar{K}^{*0} mass [8]. This wider window leads to a larger fraction of combinatorial background than in the $D_s^+ \rightarrow \phi\pi^+$ mode. To reduce this background, we require $|\cos\theta_H| > 0.5$. In addition, substantial background arises from the decays $D^+ \rightarrow \bar{K}^{*0}\pi^+$ and $D^+ \rightarrow \bar{K}^0\pi^+$, which tend to peak around the nominal D_s^+ mass if the pion is misidentified as a kaon. This background is suppressed by requiring that the kaon daughter of the \bar{K}^{*0} satisfy the loose kaon identification criterion and the other kaon, the tight criterion.

For the decay mode $D_s^+ \rightarrow K_s^0K^+$, with $K_s^0 \rightarrow \pi^+\pi^-$, the $\pi^+\pi^-$ invariant mass must be within $15 \text{ MeV}/c^2$ of the nominal K_s^0 mass [8], and the charged kaon must satisfy the tight criterion. To improve the purity of the K_s^0 sample, we require the angle α between the K_s^0 momentum vector and the K_s^0 flight direction to satisfy $\cos\alpha > 0.98$.

The invariant mass M_{D_s} of D_s^+ candidates is required to be within three standard deviations (σ_{D_s}) of the signal distribution peak $M_{D_s}^{\text{peak}}$ seen in the data.

D_s^+ candidates satisfying these selection criteria are combined with photon candidates to form $D_s^{*+} \rightarrow D_s^+\gamma$ candidates. Candidate photons are required to satisfy $E_\gamma > 50 \text{ MeV}$, where E_γ is the photon energy in the laboratory frame, and $E_\gamma^* > 110 \text{ MeV}$, where E_γ^* is the photon energy in the CM frame. When the photon candidate is combined with any other photon candidate in the event, the pair must not form a good π^0 candidate, defined by a total CM energy $E_{\gamma\gamma}^* > 200 \text{ MeV}$ and an invariant mass $115 < M_{\gamma\gamma} < 155 \text{ MeV}/c^2$.

The D_s^{*+} candidates must satisfy $|\Delta M - \Delta M^{\text{peak}}| < 2.5\sigma_{\Delta M}$, where ΔM^{peak} is the peak of the signal $\Delta M = M(D_s^+\gamma) - M(D_s^+)$ distribution observed in the data. The CM momentum of the $D_s^{(*)+}$ candidate is required to be greater than $1.5 \text{ GeV}/c$.

$D_s^{(*)+}$ candidates are combined with π^- candidates to form partially reconstructed $B^0 \rightarrow D_s^{(*)+}D^{*-}$ candidates. Since the transverse momentum of the pion in

signal events is less than $210 \text{ MeV}/c$, these tracks are not required to have DCH hits.

Due to the high combinatorial background in the ΔM distribution, more than one $D_s^{*+}\pi^-$ candidate pair is found per event, with about a 20% probability from signal Monte Carlo simulation. To select the best candidate in the event, the following χ^2 is calculated for each D_s^{*+} candidate

$$\chi^2 = [(M_i - M_i^{\text{peak}})/\sigma_i]^2 + [(M_{D_s} - M_{D_s}^{\text{peak}})/\sigma_{D_s}]^2 + [(\Delta M - \Delta M^{\text{peak}})/\sigma_{\Delta M}]^2, \quad (2)$$

where M_i is the measured invariant mass of the intermediate $i = \phi, K^{*0},$ or K_s^0 candidate, depending on the D_s^+ decay mode, M_i^{peak} is the corresponding peak of the signal M_i distribution, and σ_i is its width obtained from data. The candidate with the smallest value of χ^2 in the event is retained.

V. RESULTS

The missing mass distributions of candidates for partially reconstructed $B^0 \rightarrow D_s^{(*)+}D^{*-}$ decays are shown in Fig. 1. A clear signal peak is observed in all modes. We perform a binned maximum likelihood fit to these distributions. The fit function is the sum of a Gaussian distribution and a background function given by

$$f_B(M_{\text{miss}}) = \frac{C_1(M_0 - M_{\text{miss}})^{C_2}}{C_3 + (M_0 - M_{\text{miss}})^{C_2}}, \quad (3)$$

where C_i are parameters determined by the fit, and $M_0 \equiv M_{D^{*-}} - M_\pi = 1.871 \text{ GeV}/c^2$ is the kinematic end point. The fits find 3704 ± 232 and 1493 ± 95 events under the Gaussian peak in the sum of the $D_s^+\pi^-$ and $D_s^{*+}\pi^-$ distributions, respectively. However, due to the presence of cross feed and self-cross feed, discussed below, further analysis is needed in order to extract the signal yields and the branching fractions.

We use a Monte Carlo simulation, which includes both $B\bar{B}$ and $q\bar{q}$ continuum events, to study the missing mass distributions of the different background sources. We consider two kinds of backgrounds: a peaking component that contributes predominantly at the end of the missing mass distribution in the signal region and a non-peaking component that is more uniform. The non-peaking component is well modeled by the background function (3). The peaking component receives contributions from related channels due to

- **Cross Feed (CF):** if the soft photon from a $D_s^{*+} \rightarrow D_s^+\gamma$ decay is not reconstructed, $B^0 \rightarrow D_s^{*+}D^{*-}$ decays may lead to an enhancement under the signal peak of the $D_s^+\pi^-$ missing mass spectrum. Similarly, $B^0 \rightarrow D_s^+D^{*-}$ decays may lead to

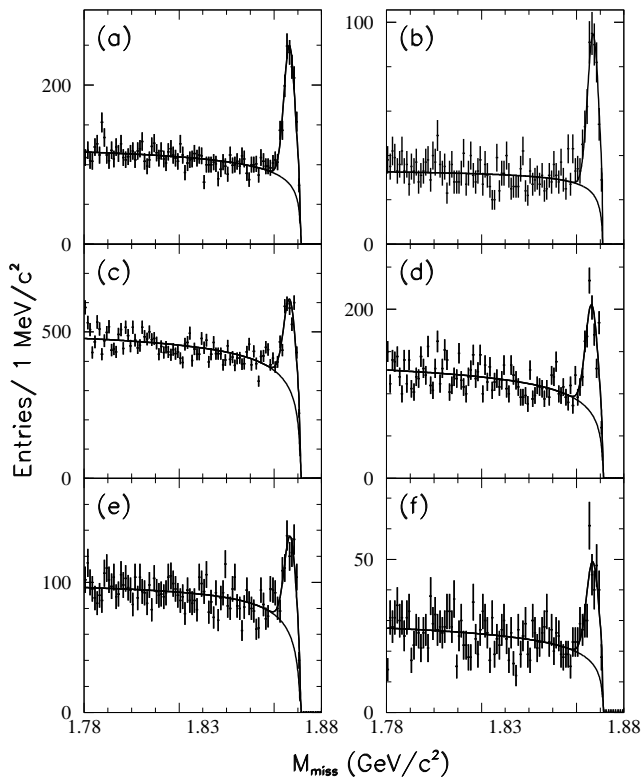


FIG. 1: Missing mass distributions of B candidates in data. (a) $D_s^+ \pi^-$ with $D_s^+ \rightarrow \phi \pi^+$, (b) $D_s^{*+} \pi^-$ with $D_s^+ \rightarrow \phi \pi^+$, (c) $D_s^+ \pi^-$ with $D_s^+ \rightarrow \bar{K}^{*0} K^+$, (d) $D_s^{*+} \pi^-$ with $D_s^+ \rightarrow \bar{K}^{*0} K^+$, (e) $D_s^+ \pi^-$ with $D_s^+ \rightarrow K_S^0 K^+$, (f) $D_s^{*+} \pi^-$ with $D_s^+ \rightarrow K_S^0 K^+$. The curves show the result of the fit (see text), indicating the signal and background contributions.

a peaking enhancement in the $D_s^{*+} \pi^-$ M_{miss} spectrum, due to the combination of a D_s^+ with a random photon.

- **Self-Cross Feed (SCF):** this is due to true $B^0 \rightarrow D_s^{*+} D^{*-}$ decays in which the D_s^+ is correctly reconstructed, but combined with a random photon to produce the wrong D_s^{*+} candidate, resulting in a peaking enhancement in the $D_s^{*+} \pi^-$ spectrum.

Table I presents the reconstruction efficiency of correctly reconstructed signal $B^0 \rightarrow D_s^{(*)+} D^{*-}$ decays, as well as cross feed and self-cross feed, found for simulated events in the signal region $M_{\text{miss}} > 1.86 \text{ GeV}/c^2$.

In addition to these background sources, we also considered a possible contribution from the charged and neutral B decays $B \rightarrow D_s^{(*)+} \bar{D}^{**}$. These potential background sources were simulated with four \bar{D}^{**} states: the observed $\bar{D}_1(2420)$ and $\bar{D}_2^*(2460)$ mesons, and the $\bar{D}_0^*(j=1/2)$ and $\bar{D}_1(j=1/2)$ mesons predicted by HQET [9]. Their contribution was determined to be negligible, mainly due to the $D_s^{(*)+}$ CM momentum cut.

TABLE I: Efficiencies for $B^0 \rightarrow D_s^{(*)+} D^{*-}$ decay modes to contribute to the $D_s^+ \pi^-$ and $D_s^{*+} \pi^-$ missing mass distributions in the signal region $M_{\text{miss}} > 1.86 \text{ GeV}/c^2$. Two different $B^0 \rightarrow D_s^{*+} D^{*-}$ Monte Carlo samples have been used, one with longitudinal (long.) and the other with transverse (transv.) polarization.

| Generated mode | Reconstructed mode | |
|---|--------------------|-------------------|
| | $D_s^+ \pi^-$ | $D_s^{*+} \pi^-$ |
| $B^0 \rightarrow D_s^+ D^{*-}$ | $(23.6 \pm 1.0)\%$ | $(1.7 \pm 0.3)\%$ |
| $B^0 \rightarrow D_s^{*+} D^{*-}$ (long.) | $(9.0 \pm 0.3)\%$ | $(7.4 \pm 0.3)\%$ |
| Self-Cross Feed | | $(1.6 \pm 0.1)\%$ |
| $B^0 \rightarrow D_s^{*+} D^{*-}$ (transv.) | $(10.4 \pm 0.3)\%$ | $(6.9 \pm 0.3)\%$ |
| Self-Cross Feed | | $(1.4 \pm 0.1)\%$ |

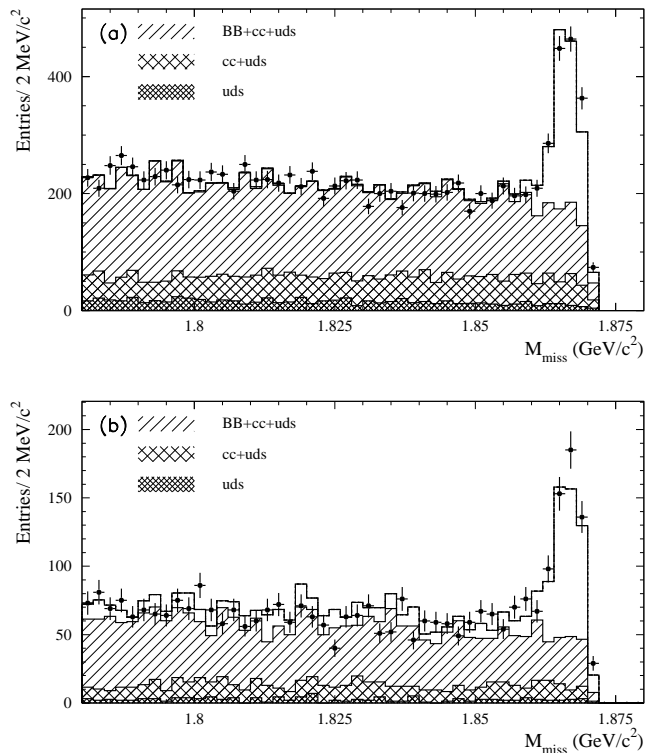


FIG. 2: Missing mass distribution for (a) $D_s^+ \pi^-$ and (b) $D_s^{*+} \pi^-$ combinations for data (points with error bars) and Monte Carlo (histogram). The contributions from the $B\bar{B}$, $c\bar{c}$ and $q\bar{q}$ with $q = u, d, s$ (labeled uds in the figure) are shown separately. The cross feed and self-cross feed backgrounds are included in the total histogram, but not in the hatched $B\bar{B}$ histogram.

Multi-body decays $B \rightarrow D_s^{(*)+} X$ are found not to contribute due to the same cut.

Figure 2 shows a comparison of the missing mass distributions in data and Monte Carlo simulation. We assume 1.05% and 1.59% branching fractions for the $B^0 \rightarrow D_s^+ D^{*-}$ and $B^0 \rightarrow D_s^{*+} D^{*-}$ decays, respectively, in the Monte Carlo simulation.

The number of events in the peaks in the $D_s^+\pi^-$ and $D_s^{*+}\pi^- M_{\text{miss}}$ distributions is obtained from the fits described above. The branching fractions are computed from these yields correcting for cross feed and self-cross feed background. This is done by inverting the 2×2 efficiency matrix, whose diagonal elements correspond to the sum of signal and self-cross feed efficiencies presented in Table I, and whose off-diagonal terms are the cross-feed efficiencies. The efficiencies corresponding to transverse and longitudinal polarization of $B^0 \rightarrow D_s^{*+}D^{*-}$ have been weighted according to the measured polarization discussed below. With this procedure, the $B^0 \rightarrow D_s^{*+}D^{*-}$ branching fractions are determined to be

$$\mathcal{B}(B^0 \rightarrow D_s^+D^{*-}) = (1.03 \pm 0.14 \pm 0.13 \pm 0.26)\%, \quad (4)$$

$$\mathcal{B}(B^0 \rightarrow D_s^{*+}D^{*-}) = (1.97 \pm 0.15 \pm 0.30 \pm 0.49)\%, \quad (5)$$

and their sum is

$$\mathcal{B}(B^0 \rightarrow D_s^{(*)+}D^{*-}) = (3.00 \pm 0.19 \pm 0.39 \pm 0.75)\%, \quad (6)$$

where the first error is statistical, the second is the systematic error from all sources other than the uncertainty in the $D_s^+ \rightarrow \phi\pi^+$ branching fraction, and the third error, which is dominant, is due the uncertainty in the $D_s^+ \rightarrow \phi\pi^+$ branching fraction $\mathcal{B}(D_s^+ \rightarrow \phi\pi^+) = (3.6 \pm 0.9)\%$ [8]. Correlations in the systematic errors between Eqs. (4) and (5) are taken into account in Eq. (6). The sources of the systematic error are discussed in Sec. VI.

The measurement of the fraction of the longitudinal polarization Γ_L/Γ in the $B^0 \rightarrow D_s^{*+}D^{*-}$ decay mode is performed for candidates having missing mass in the signal region ($M_{\text{miss}} > 1.86 \text{ GeV}/c^2$). To minimize the systematic error due to large backgrounds, the polarization measurement involves only the $D_s^+ \rightarrow \phi\pi^+$ channel, which has the best signal to background ratio. Two angles are used: the helicity angle θ_γ between the D^{*-} and the soft photon direction in the D_s^{*+} rest frame, and the helicity angle θ_π between the D_s^{*+} and the soft pion direction in the D^{*-} rest frame. Since the B meson is not fully reconstructed, we compute θ_γ and θ_π by constraining M_{miss} to the nominal D^0 mass [8] to obtain a unique solution for the azimuth ϕ .

The two-dimensional distribution $(\cos\theta_\gamma, \cos\theta_\pi)$ is divided into five ranges in each dimension, resulting in 25 bins. The combinatorial background, as well as the cross feed and the self-cross feed obtained from Monte Carlo simulation, are subtracted from this two-dimensional data distribution. The resulting signal distribution is corrected bin-by-bin for detection efficiency, which is obtained from the simulation separately for each bin. A two-dimensional binned minimum- χ^2 fit is then performed to the efficiency-corrected signal distribution with the fit function

$$\frac{d^2\Gamma}{d\cos\theta_\pi d\cos\theta_\gamma} \propto \frac{\Gamma_L}{\Gamma} \cos^2\theta_\pi \sin^2\theta_\gamma + (1 - \frac{\Gamma_L}{\Gamma}) \sin^2\theta_\pi \frac{1 + \cos^2\theta_\gamma}{4}. \quad (7)$$

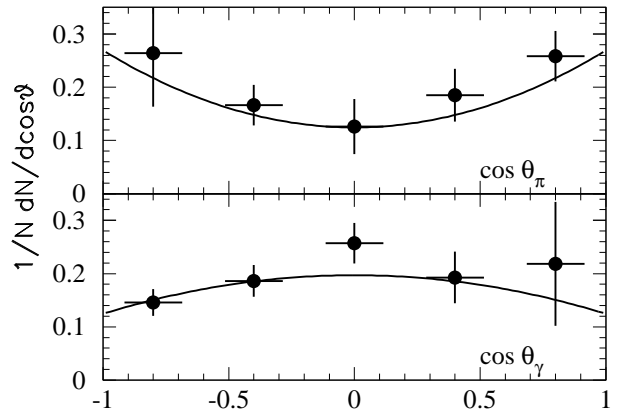


FIG. 3: Projections of the number of background-subtracted data events on the $\cos\theta_\pi$ and $\cos\theta_\gamma$ axes. The result of the two-dimensional fit is overlaid.

The resulting fit has a χ^2 of 23.1 for 25 bins with two floating parameters (Γ_L/Γ and total normalization). Figure 3 shows the data and the result of the fit projected on the $\cos\theta_\gamma$ and $\cos\theta_\pi$ axes.

From the fit, the fraction of longitudinal polarization is determined to be

$$\Gamma_L/\Gamma = (51.9 \pm 5.0 \pm 2.8)\%, \quad (8)$$

where the first error is statistical and the second is systematic.

VI. SYSTEMATIC UNCERTAINTIES

The various contributions to the systematic errors on the branching fraction and polarization measurements are summarized in Table II. The dominant systematic error for the branching fractions is the uncertainty on the three D_s^+ branching fractions. To evaluate the uncertainty due to the background subtraction, the signal yield is determined using an alternative method in which the number of events is extracted directly from the histogram after subtraction of the background, which is estimated with the Monte Carlo simulation. The difference of the signal yields obtained in this way from the results of the fit was taken as a systematic error. This also accounts for the systematic error due to a possible deviation of the signal shape from a Gaussian.

The Monte Carlo statistical errors in the determination of the signal and the cross feed efficiencies are included as a systematic error. The uncertainty in the calculation of the $B^0 \rightarrow D_s^{*+}D^{*-}$ polarization is propagated to the branching fraction systematic error. The systematic error due to the uncertainty on the efficiency for the reconstruction of charged particles is 1.2% times the number of charged particles in the decay. An additional error of 1.6% is added in quadrature to account for the uncertainty in the reconstruction efficiency of the soft pion.

TABLE II: Sources of systematic uncertainties (%) for the $B^0 \rightarrow D_s^{(*)+} D^{*-}$ branching fractions and $B^0 \rightarrow D_s^{*+} D^{*-}$ polarization measurements.

| Source | $D_s^+ D^{*-}$ | $D_s^{*+} D^{*-}$ | $\sigma(\Gamma_L/\Gamma)$ |
|--|----------------|-------------------|---------------------------|
| Background subtraction or modeling | 2.7 | 5.9 | 0.5 |
| Monte Carlo statistics | 4.2 | 6.0 | 2.7 |
| Polarization uncertainty | 0.8 | 0.5 | - |
| Cross feed | 3.2 | 2.4 | - |
| Number of B pairs | 1.6 | 1.6 | - |
| $\mathcal{B}(\phi \rightarrow K^+ K^-)$ | 1.6 | 1.6 | - |
| Particle identification | 1.0 | 1.0 | 0.1 |
| Tracking efficiency | 3.6 | 3.6 | 0.5 |
| Soft pion efficiency | 2.0 | 2.0 | 0.2 |
| Relative branching fractions | 10.2 | 10.2 | - |
| $\mathcal{B}(D_s^{*+} \rightarrow D_s^+ \gamma)$ | - | 2.7 | - |
| Photon efficiency | - | 1.3 | 0.1 |
| π^0 veto | - | 2.7 | 0.3 |
| Total systematic error | 13.1 | 15.1 | 2.8 |

The systematic error due to the π^0 veto requirement was studied by measuring the relative D_s^{*+} yields in data and Monte Carlo with and without the π^0 veto.

In the polarization measurement, the level of the various backgrounds depends on the charged track, neutral cluster, and particle identification efficiencies. The fit was repeated varying the background according to the errors in these efficiencies, and the resulting variations in Γ_L/Γ were taken as the associated systematic error.

TABLE III: The fractional difference $\langle(N_D - N_{MC})/N_{MC}\rangle$, averaged over all M_{miss} bins, where N_D (N_{MC}) is the number of data (Monte Carlo) candidates in a given bin of the M_{miss} distribution of the given control sample. SB (SR) refers to the M_{D_s} or ΔM sideband (signal region) control sample. WS indicates wrong sign $D_s^{(*)+} \pi^+$ combinations, and $-p_{D_s^{(*)+}}^*$ indicates that M_{miss} was calculated from the negative of the $D_s^{(*)+}$ CM momentum. The missing mass range $1.78 < M_{\text{miss}} < 1.87 \text{ GeV}/c^2$ is used for the control sample, except for the first line.

| Sample type | $D_s^+ \pi^-$ | $D_s^{*+} \pi^-$ |
|---|--------------------|--------------------|
| $1.78 < M_{\text{miss}} < 1.85 \text{ GeV}/c^2$ | -0.009 ± 0.007 | 0.075 ± 0.014 |
| SB | -0.075 ± 0.006 | 0.007 ± 0.022 |
| SR, WS | 0.006 ± 0.008 | 0.044 ± 0.015 |
| SB, WS | -0.060 ± 0.007 | -0.008 ± 0.024 |
| SR, $-p_{D_s^{(*)+}}^*$ | 0.015 ± 0.009 | 0.075 ± 0.016 |
| SB, $-p_{D_s^{(*)+}}^*$ | -0.062 ± 0.007 | -0.123 ± 0.022 |
| Average | -0.038 ± 0.003 | 0.032 ± 0.007 |

To check that the simulation accurately reproduces

the background M_{miss} distributions in the data, a thorough data-Monte Carlo comparison is made in control samples containing no signal events. These samples are events with $1.78 < M_{\text{miss}} < 1.85 \text{ GeV}/c^2$; events in the D_s^+ sideband $1.89 < M_{D_s} < 1.95 \text{ GeV}/c^2$ or $1.985 < M_{D_s} < 2.05 \text{ GeV}/c^2$; events in the D_s^{*+} sideband $170 < \Delta M < 300 \text{ MeV}/c^2$; wrong sign $D_s^{(*)+} \pi^+$ combinations in either the M_{D_s} and ΔM sidebands or signal regions determined above; and candidates in which M_{miss} was calculated with the inverse of the $D_s^{(*)+}$ center-of-mass momentum $p_{D_s^{(*)+}}^*$. The comparison between data and Monte Carlo simulation for these control samples is shown in Table III. The average level of discrepancy is used to estimate the uncertainty in the modeling of the background.

VII. SUMMARY

In summary, based on a partial reconstruction technique, we have measured the branching fractions

$$\mathcal{B}(B^0 \rightarrow D_s^+ D^{*-}) = (1.03 \pm 0.14 \pm 0.13 \pm 0.26)\% ,$$

$$\mathcal{B}(B^0 \rightarrow D_s^{*+} D^{*-}) = (1.97 \pm 0.15 \pm 0.30 \pm 0.49)\% ,$$

$$\mathcal{B}(B^0 \rightarrow D_s^{(*)+} D^{*-}) = (3.00 \pm 0.19 \pm 0.39 \pm 0.75)\% .$$

The fraction of the longitudinal D_s^{*+} polarization in $B^0 \rightarrow D_s^{*+} D^{*-}$ decays is determined to be

$$\Gamma_L/\Gamma = (51.9 \pm 5.0 \pm 2.8)\% .$$

This measurement is consistent with theoretical predictions assuming factorization, which range from 50 to 55% [10, 11]. Our results are also in good agreement with previous experimental results [3, 6].

VIII. ACKNOWLEDGMENTS

We are grateful for the excellent luminosity and machine conditions provided by our PEP-II colleagues, and for the substantial dedicated effort from the computing organizations that support BABAR. The collaborating institutions wish to thank SLAC for its support and kind hospitality. This work is supported by DOE and NSF (USA), NSERC (Canada), IHEP (China), CEA and CNRS-IN2P3 (France), BMBF and DFG (Germany), INFN (Italy), NFR (Norway), MIST (Russia), and PPARC (United Kingdom). Individuals have received support from the A. P. Sloan Foundation, Research Corporation, and Alexander von Humboldt Foundation.

-
- [1] M. Bauer, B. Stech, M. Wirbel, *Z. Phys. C* **34**, 103 (1987).
- [2] CLEO Collaboration, M. S. Alam *et al.*, *Phys. Rev. D* **50**, 43 (1994).
- [3] CLEO Collaboration, D. Gibaut *et al.*, *Phys. Rev. D* **53**, 4734 (1996).
- [4] CLEO Collaboration, G. Bonvicini *et al.*, CLEO CONF 98-23, presented at the 29th International Conference on High Energy Physics, Vancouver, Canada (1998).
- [5] CLEO Collaboration, J. P. Alexander *et al.*, *Phys. Rev. D* **64**, 092001 (2001).
- [6] CLEO Collaboration, S. Ahmed *et al.*, *Phys. Rev. D* **62**, 112003 (2000).
- [7] BABAR Collaboration, A. Palano *et al.*, *Nucl. Instr. Meth. A* **479**, 1 (2002).
- [8] Particle Data Group, K. Hagiwara *et al.*, *Phys. Rev. D* **66**, 010001 (2002).
- [9] A. F. Falk and M. Luke, *Phys. Lett. B* **292**, 119 (1992).
- [10] J. D. Richman, in *Probing the Standard Model of Particle Interactions*, edited by R. Gupta, A. Morel, E. de Rafael, and F. David (Elsevier, Amsterdam, 1999), p.640.
- [11] Z. Luo and J. L. Rosner, *Phys. Rev. D* **64**, 094001 (2001).